



HAL
open science

On the mechanical properties and auxetic potential of various organic networked polymers

Joseph N Grima, Daphne Attard, Richard Nicholas Cassar, Luke Farrugia, Lara Trapani, Ruben Gatt

► **To cite this version:**

Joseph N Grima, Daphne Attard, Richard Nicholas Cassar, Luke Farrugia, Lara Trapani, et al.. On the mechanical properties and auxetic potential of various organic networked polymers. *Molecular Simulation*, 2008, 34 (10-15), pp.1149-1158. 10.1080/08927020802512187 . hal-00515061

HAL Id: hal-00515061

<https://hal.science/hal-00515061>

Submitted on 4 Sep 2010

HAL is a multi-disciplinary open access archive for the deposit and dissemination of scientific research documents, whether they are published or not. The documents may come from teaching and research institutions in France or abroad, or from public or private research centers.

L'archive ouverte pluridisciplinaire **HAL**, est destinée au dépôt et à la diffusion de documents scientifiques de niveau recherche, publiés ou non, émanant des établissements d'enseignement et de recherche français ou étrangers, des laboratoires publics ou privés.

On the mechanical properties and auxetic potential of various organic networked polymers

| | |
|---|---|
| Journal: | <i>Molecular Simulation/Journal of Experimental Nanoscience</i> |
| Manuscript ID: | GMOS-2008-0054.R1 |
| Journal: | Molecular Simulation |
| Date Submitted by the Author: | 13-Sep-2008 |
| Complete List of Authors: | Grima, Joseph; University of Malta, Department of Chemistry Attard, Daphne; University of Malta Cassar, Richard; University of Malta Farrugia, Luke; University of Malta Trapani, Lara; University of Malta Gatt, Ruben; University of Malta |
| Keywords: | auxetic, mechanical properties, negative Poisson's ratio |
| Note: The following files were submitted by the author for peer review, but cannot be converted to PDF. You must view these files (e.g. movies) online. | |
| anim.rar | |

SCHOLARONE™
Manuscripts

Grima, Attard *et al.* (2008)

On the mechanical properties and auxetic potential of various organic networked polymers

Joseph N. Grima, Daphne Attard, Richard N. Cassar, Luke Farrugia, Lara Trapani and Ruben Gatt

Department of Chemistry, University of Malta, Msida, MSD 2080, Malta

e-mail: joseph.grima@um.edu.mt - www: <http://home.um.edu.mt/auxetic>

We simulate and analyse three types of 2-D networked polymers which had been predicted to exhibit on-axis auxetic behaviour (negative Poisson's ratio), namely (i) polyphenylacetylene networks which behave like flexing re-entrant honeycombs, commonly referred to as 'reflexynes', (ii) polyphenylacetylene networks that mimic the behaviour of rotating triangles, commonly referred to as 'polytriangles' and (iii) networked polymers built from calix[4]arene units. More specifically, we compute and compare their in-plane off-axis mechanical behaviour, in particular their off-axis Poisson's ratios and show that in some cases, the sign and magnitude of Poisson's ratio is dependent on the direction of loading. We propose two functions which can provide a measure for the extent of auxeticity for such anisotropic materials and show that the polytriangles are predicted as the most auxetic when compared to the other networks with the reflexyne re-entrant networks being the least auxetic.

Keywords: auxetic; negative Poisson's ratios; mechanical properties; networked polymers

1
2
3
4
5
6
7
8
9
10
11
12
13
14
15
16
17
18
19
20
21
22
23
24
25
26
27
28
29
30
31
32
33
34
35
36
37
38
39
40
41
42
43
44
45
46
47
48
49
50
51
52
53
54
55
56
57
58
59
60

Grima, Attard *et al.* (2008)

1. Introduction

Materials with negative Poisson's ratios, more commonly known as auxetics [1], exhibit the anomalous property of expanding laterally when stretched and contracting laterally when compressed [1,2]. This behaviour is in sharp contrast to that of 'normal' everyday (conventional) materials for which the Poisson's ratio is positive with a value usually lying within the range 0.25-0.33 [3].

Although auxetics are not commonly encountered in everyday life, in recent years there has been considerable research into this field in view of their very useful properties [4]. This led to the discovery of numerous auxetic materials [1,2,5-41], ranging from synthetic polymeric foams [10-16] to naturally occurring silicates and zeolites [17-31]. Additionally, a number of auxetic models and structures have also been identified [42-56].

In all of the above cases, auxeticity can be explained in terms of the geometry of the system and the way this geometry changes when the system is subjected to uniaxial loads (deformation mechanism). For example, the Poisson's ratios in the naturally occurring silicate α -cristobalite and in various zeolites have been explained using models based on connected rigid units which, when loaded in tension, rotate relative to each other to form a more open structure [27,28,42,50], whilst the auxeticity in the liquid-crystalline polymers synthesised by Griffin *et al.* have been attributed to a model involving the rotation of laterally attached rods [33-35].

It is important to note that although naturally occurring materials have the obvious advantage that they need not be synthesised, man-made auxetics offer the benefit that their macroscopic properties may be tailor-made to exhibit a specific pre-determined profile of mechanical properties thus making them better suited for

1 Grima, Attard *et al.* (2008)

2
3 particular applications. One approach for designing man-made molecular-level
4 auxetics is to have a molecular structure that mimics the properties of another auxetic
5 system, for example, a naturally occurring auxetic or an auxetic macrostructure.
6
7
8
9
10 Downscaling of macrostructures to the molecular level, a technique first used in the
11 pioneering work by Evans *et al.* [1], is possible because the Poisson's ratio is a scale
12 independent property, i.e. the Poisson's ratio is normally unaffected by the scale at
13 which a particular 'deformation mechanism' operates. In this respect, it should be
14 noted that if a geometry-based model for the behaviour of a system is available, then
15 this model can be used as a guide for fine-tuning the design and synthesis of
16 molecular auxetics.
17
18
19
20
21
22
23
24
25
26
27
28

29 In this paper we use the commercially available molecular modelling package
30 Materials Studio V4.2 (Accelrys Inc., San Diego, USA) to re-examine a number of
31 'auxetic' 2D molecular networks which have been designed through the downscaling
32 technique, namely:
33
34
35
36
37

- 38 (1) 'reflexyne' polyphenylacetylene networks (see Fig. 1a), originally reported by
39 Evans *et al.* [1] which mimic the behaviour of auxetic re-entrant honeycombs
40 (Fig 2a),
41
42
43
44
- 45 (2) 'polytriangles' polyphenylacetylene networks (see Fig. 1b), originally reported
46 by Grima and Evans [6] which mimic the behaviour of rotating triangles (Fig.
47 2b), and
48
49
50
51
- 52 (3) polymers built from calix[4]arenes (see Fig. 1c) (henceforth referred to as
53 'polycalixes'), originally reported by Grima *et al.* [7,8] that mimic the
54 behaviour of an 'egg rack' macrostructure which when loaded in tension, opens
55
56
57
58
59
60

1
2
3
4
5
6
7
8
9
10
11
12
13
14
15
16
17
18
19
20
21
22
23
24
25
26
27
28
29
30
31
32
33
34
35
36
37
38
39
40
41
42
43
44
45
46
47
48
49
50
51
52
53
54
55
56
57
58
59
60

Grima, Attard *et al.* (2008)

up in all directions like an umbrella (Fig. 2c & d), hence producing a negative Poisson's ratio in the plane of the structure.

In particular, we assess how these systems behave when they are loaded in an in-plane off-axis direction in an attempt to determine which of these systems is most capable of exhibiting auxetic behaviour.

- Insert Fig. 1 -

- Insert Fig. 2 -

-- Note that Fig. 2a-c is also provided in the form of animations --

2. Simulations

Force-field based simulations were carried out using the commercially available software package Materials Studio, V4.2 (Accelrys Inc., San Diego, USA) on nine systems illustrated in Fig. 1, in particular three reflexynes (**1A–C**, see Fig. 1a with $(m,n) = (1,4), (1,5)$ and $(1,6)$ respectively), three polytriangles (**2A–C**, see Fig. 1b with $n = 3, 4$ and 5 respectively) and three polycalixes (**3A–C**, see Fig. 1c with $n = 0, 1$ and 2 respectively). These systems, which have all been modelled before using different force-fields in an attempt to obtain their on-axis Poisson's ratio and Young's moduli [5-6, 8-9] have been chosen as they represent a representative sample of each class of materials.

1 Grima, Attard *et al.* (2008)

2
3 These systems were build as infinite crystalline systems (see Fig. 1) with the plane of
4 interest aligned in the (100) plane. In the third direction, the networks were allowed to
5 stack freely ‘on each other’ (in the case of the reflexynes and the polytriangles) or
6
7
8
9
10
11
12
13
14
15
16
17
18
19
20
21
22
23
24
25
26
27
28
29
30
31
32
33
34
35
36
37
38
39
40
41
42
43
44
45
46
47
48
49
50
51
52
53
54
55
56
57
58
59
60
These systems were build as infinite crystalline systems (see Fig. 1) with the plane of interest aligned in the (100) plane. In the third direction, the networks were allowed to stack freely ‘on each other’ (in the case of the reflexynes and the polytriangles) or ‘inside one another’ (in the case of the polycalixes). The crystals were oriented in the global XYZ space in such a way that the [001] direction was always parallel to the Z -axis with the [010] direction lying in the YZ -plane. This alignment was chosen so as to ensure that the plane of the networks remains parallel to the YZ -plane and to enable a direct comparison with earlier work by Grima *et al.* [6-8] performed using Cerius² (Accelerys Inc., San Diego, USA).

Energy expressions for each of these nine networks were set up through the Discover Simulation Engine within Materials Studio 4.2 (henceforth referred to as MS Discover) using parameters from the PCFF [57] force-field¹ with non-bond terms being added using the Ewald summation technique [58]. Note that the PCFF force-field was chosen in preference to the DREIDING force-field which was used in the earlier studies on the reflexynes [9] and the polytriangles [6] in view of the fact that unlike the PCFF force-field, the DREIDING force-field is unable to correctly represent the C_{4v} symmetry which is characteristic of single calix[4]arenes.

An energy minimisation was then performed to the default MS Discover ultra-fine convergence criteria using the SMART minimiser as implemented in MS Discover². During the minimisation, all cell parameters were set as variables, i.e. no constraints on the shape and size of the unit cell were applied.

¹As shown in Table 1, the PCFF force-field can simulate all the systems under consideration allowing for a proper and unbiased comparison between the systems, as discussed later.

² The SMART minimiser as implemented within MS Discover is a compound minimiser where the minimisation commences with the steepest descent algorithm followed by a conjugate gradient algorithm and terminates with a Newton Raphson algorithm.

Grima, Attard *et al.* (2008)

The 6x6 stiffness matrix \mathbf{C} , which relates the stress $\boldsymbol{\sigma}$ and the strain $\boldsymbol{\varepsilon}$ through $\boldsymbol{\sigma} = \mathbf{C} \boldsymbol{\varepsilon}$, was then simulated using the constant strain method found in the Materials Studio V 4.2 Forcite module (henceforth referred to as MS Forcite). In these simulations, the maximum strain amplitude was set to 0.003 i.e. 0.3% strain and 7 distorted structures were generated for each strain pattern. Note that in such simulations, the maximum strain amplitude should be in the range of 0.1 - 1% in an attempt to ensure that the strains are small enough to permit the structure to behave within its region of linear elasticity and at the same time avoid a situation where the strains are so low that the simulations generate a set of structures that are very similar to one another, in which case computational noise may become significant when comparing their calculated stress values.

The in-plane on-axis Poisson's ratios and moduli from these systems were then calculated from the compliance matrix $\mathbf{S} = \mathbf{C}^{-1}$ which for the YZ plane (the plane of the networks) are given by:

$$\text{Young's moduli : } E_y = \frac{1}{s_{22}} \quad E_z = \frac{1}{s_{33}}$$

$$\text{Poisson's ratios: } \nu_{yz} = -s_{32}E_y = -\frac{s_{32}}{s_{22}} \quad \nu_{zy} = -s_{23}E_z = -\frac{s_{23}}{s_{33}}$$

$$\text{Shear moduli: } G_{yz} = \frac{1}{s_{44}}$$

whilst the off-axis properties can be obtained after the stiffness matrices are transformed using appropriate axis transformation techniques [59].

Grima, Attard *et al.* (2008)

Results and Discussion

(a) The simulated structures at zero stress

The simulations suggest that the minimum energy conformations of all the molecular network models possess a shape which is similar to the idealised structure which they are meant to mimic (see Fig. 3). We note that in all systems, the favourable π - π interactions between the different layers are being well represented. In fact, for polyphenylacetylene networks, the minimum energy separation between the different layers down the third direction is approx. 3.28Å in the case of the reflexynes (see Fig. 3a) and approx. 3.44Å in the case of polytriangles (see Fig. 3b), whilst, in the polycalixes we find that, for example, the distance between parallel layers of calix[4]arenes in **3A** is 3.38Å (see Fig. 3c). These separations are comparable to the distance between layers of graphite (3.35Å) [60]. We also note that in general, stacking in the third dimension is in such a way that whenever possible, the centres of the benzene rings are off-set from one another, this being clearly indicated by the deviations in the unit cell angles β and γ from 90° in the case of the polyphenylacetylene networks (see Fig. 4). It is also interesting to note that the (1,4)-reflexyne molecular network **1A** is significantly non-planar with the phenyl rings adopting a conformation where they are at an angle to the YZ-plane (the ‘plane of the networks’) as illustrated in Fig. 3a, once again, in an attempt to optimise the favourable π - π interactions between the spatially adjacent phenyl rings in the system.

- Insert Fig. 3 -

- Insert Fig. 4-

1 Grima, Attard *et al.* (2008)

2
3
4 *(b) The simulated on-axis Poisson's ratios and moduli*

5 The on-axis Poisson's ratios and moduli as simulated in this study by the PCFF force-
6 field are summarised in Table 1 where they are compared with the equivalent
7 published data obtained using the DREIDING force-field in the case of the reflexynes
8 [5,9] and polytriangles [6] and the PCFF force-field found within Cerius² in the case
9 of the polycalixes [8].
10
11
12
13
14
15
16
17
18
19

20 - Insert Table 1 -
21
22
23

24 When analysing these results, we note that in the case of the polycalixes, the
25 simulations carried out by Materials Studio were in excellent agreement with the
26 simulations performed using the same force-field as found in Cerius², thus confirming
27 that the mechanical properties calculation tools found in the Forcite module of
28 Materials Studio are well implemented. The small deviations obtained are to be
29 expected in view of the fact that the energy minimisation process depends on both the
30 minimisation algorithm chosen and on the initial direction that the minimiser takes,
31 and thus minor differences can arise when a minimisation is repeated.
32
33
34
35
36
37
38
39
40
41
42
43
44
45

46 In the case of the polyphenylacetylene networks **1A-C** and **2A-C**, we note that our
47 simulations confirm the predictions made in the previous studies using the
48 DREIDING force-field that all of these systems exhibit negative on-axis Poisson's
49 ratios in the plane of the networks (the *YZ*-plane). It is also interesting to note that
50 although for a given structure, the different force-fields fail to agree on the actual
51 values of the Poisson's ratios, a result which could be expected given that the
52 properties are being calculated using different force-fields, the main trends in the
53
54
55
56
57
58
59
60

1 Grima, Attard *et al.* (2008)

2
3 results are still being represented, such as the observation that in the case of the
4 polytriangles, the auxeticity increases as the acetylene chains are made longer. This
5 agreement between the two sets of results is very significant as it indicates that the
6 results predicted are not artefacts of some particular force-field, thus giving additional
7 confidence in the quality of the simulated properties presented here.
8
9

10
11
12
13
14
15
16
17 When we compare the magnitude of results obtained by the different types of
18 networks, something which is now possible since the three types of networks are
19 simulated using the same force-field through the same protocol, we observe that
20 despite the differences in the geometry of the systems modelled, the results *prima*
21 *facie* suggest that all the three types of systems have a comparable potential to exhibit
22 negative **on-axis** Poisson's ratios. In fact, in all cases, the on-axis Poisson's ratio
23 ranges between -0.31 and -0.95, the actual values depending on the exact shape or
24 size of the system being modelled. For example, we find that according to the PCFF
25 force-field, ν_{zy} for **1C**, **3A** and **2A** is predicted as -0.46, -0.47 and -0.51 respectively,
26 despite the obvious differences between these systems.
27
28
29
30
31
32
33
34
35
36
37
38
39
40
41
42
43
44
45
46
47
48
49
50
51
52
53
54
55
56
57
58
59
60

If we now look at the on-axis Young's and shear moduli for the different networks we note that once again, the trends suggested by the earlier simulations are reproduced. In particular we note that in the case of the polytriangles and polycalixes, the moduli decrease as the size of the triangles or 'arm' lengths of the calixes increase (density decreases). This is expected since in general, from a mechanistic point of view, an increase in the 'arm' length leads to larger induced moments when a force is applied to the system, leading to a higher extent of deformation which is reflected in a

Grima, Attard *et al.* (2008)

1
2
3 decrease in the Young's and shear moduli. In the case of the reflexynes, the situation
4 is more complex as we find that whilst the on-axis Young's modulus in the Y -
5 direction and shear modulus increases with a decrease in n (the number of triple bonds
6 in the vertical acetylene chain aligned with the Z direction). Such variations were
7 predicted by Gibson and Ashby's mechanical model [53] (m, n in our molecular model
8 may be mapped to the variables l and h respectively in Gibson and Ashby's model).
9
10
11
12
13
14
15
16
17
18
19

20 It is also interesting to note that on-axis shear moduli of the polytriangles are
21 considerably larger than those of the other systems, a property which arises from the
22 fact that triangles are structurally difficult to shear. In this respect, it is important to
23 note that the analytical model for the idealised 'rotating hinging triangles' had
24 suggested that the shear modulus of such systems is infinite [55], a property which in
25 molecular level system is difficult to accomplish.
26
27
28
29
30
31
32
33
34
35

36 These high on-axis shear moduli are however only limited to the polytriangles. In fact
37 we find that despite the fact that re-entrant honeycombs have very high on-axis
38 Young's moduli, they are very weak in shear. For example, in the case of the
39 molecular-level honeycomb (1,4)-reflexyne (1A) G_{yz} is only 3.81 % of E_y and 4.60%
40 of E_z . The weakness of these honeycombs when subjected to an on-axis shear strain
41 is not limited to the reflexyne molecular honeycomb networks but is a property of all
42 such honeycombs, irrespective of the scale at which they are built. In fact, this
43 weakness in shear is also inferred by Gibson and Ashby's analytical equations for the
44 idealised flexing models which predict that for a flexing re-entrant honeycomb having
45 dimensions t/l and h/l of 0.01 and 2 respectively and a re-entrant angle of 30°
46
47
48
49
50
51
52
53
54
55
56
57
58
59
60

1 Grima, Attard *et al.* (2008)

2
3 (dimensions defined in Fig. 6b), the on-axis shear modulus is only 3.75% of the
4
5 Young's moduli.
6
7

8
9
10
11
12
13 *(d) The off-axis mechanical properties*

14
15 Plots of the in-plane (*YZ*-plane) off-axis Poisson's ratios and moduli for the nine
16
17 different systems are shown in Fig. 5. These plots very clearly show that because of
18
19 their distinct geometries and symmetries, the off-axis Poisson's ratio profiles of these
20
21 systems are in fact very different from each other. (Note that although there is
22
23 extensive work which discusses the on-axis properties of molecular reflexyne,
24
25 polytriangles and polycalix networks, and there is also work which discusses the off-
26
27 axis mechanical properties of idealised flexing/hinging/stretching re-entrant
28
29 honeycombs [61] and idealised 'rotating triangles' [55], no analysis of the off-axis
30
31 properties of the molecular networks has yet been presented.)
32
33
34
35
36
37
38

39 In particular, in the case of the Poisson's ratio, we observe that:

- 40
41 (1) In the case of the reflexynes, the off-axis plots are characterised by non
42
43 auxetic behaviour, having very high positive off-axis Poisson's ratios,
44
45 the maximum of which is *circa* 0.85 and corresponds approximately to
46
47 loading at 45° to the *Y*- and *Z*- directions;
48
49
50
51 (2) In the case of the polytriangles, the off-axis Poisson's ratios are always
52
53 negative and very similar to those observed on-axis (the networks are
54
55 *quasi* isotropic), as expected from systems exhibiting hexagonal
56
57 symmetry.
58
59
60

Grima, Attard *et al.* (2008)

(3) In the case of the polycalixes, the off-axis Poisson's ratios are less negative than on-axis. However, in the case of **3B** and **3C**, in-plane auxeticity can be observed for loading in any direction of the plane, and in the case of **3A**, the system is auxetic for loading in most, but not all, directions.

In an attempt to quantify these observations regarding the extent of in-plane auxeticity of the different systems, we shall define two properties, namely:

(a) The 'auxetic probability', $P_{aux}[YZ]$, a function which may be defined as:

$$P_{aux}[YZ] = \frac{1}{2\pi} \int_0^{2\pi} H_{YZ}(\zeta) d\zeta$$

where:

$$H_{YZ}(\zeta) = \begin{cases} 1 & \text{if } \nu_{yz}^{\zeta} < 0 \\ 0 & \text{if } \nu_{yz}^{\zeta} \geq 0 \end{cases}$$

which gives a measure of the probability that the in-plane Poisson's ratio is negative for loading in an arbitrary direction in the plane. This value can range from 0 to 1 where a value of 0 suggests that the system is conventional for loading in all directions whilst a value of 1 indicates that the system is auxetic for loading in all directions

(b) The 'average in-plane Poisson's ratio', $\bar{\nu}[YZ]$, which we defined as:

$$\bar{\nu}[YZ] = \frac{1}{2\pi} \int_0^{2\pi} \nu_{yz}^{\zeta} d\zeta$$

a property which gives a measure of the average Poisson's ratio in the plane.

Grima, Attard *et al.* (2008)

When these properties are evaluated for the different networks (see Table 2), we note that, starting with the most auxetic system, the order of auxeticity in the YZ -plane is:

(a) If we classify them according to the magnitude of $P_{aux} [YZ]$:

$$\{2A-C, 3B, 3C\} > 3A > 1C > 1B > 1A$$

(b) If we classify them according to the magnitude of $\bar{\nu} [YZ]$:

$$2C > 2B > 3C > 3B > 2A > 3A > 1A > 1B > 1C$$

This analysis clearly suggests that the polytriangles are the best systems in terms of the in-plane off-axis auxeticity, followed by the polycalixes and then by the reflexynes which are in fact predominantly conventional for loading off-axis.

Before we conclude our discussion on the Poisson's ratio, it is important to highlight that although the ranking above suggests that the different systems within the same class have a different extent of auxeticity, this variation is not always explainable in terms of the idealised mechanical model they are meant to mimic. For example, the idealised 'rotating triangles' model [55] predicts a constant isotropic Poisson's ratio of -1, something which is clearly not demonstrated by the molecular level model. This deviation may be explained from the fact that these molecular level networks are more complex, even in shape, when compared to the idealised model, and whilst in the idealised 'flexing rotating triangles' model, the sides of the triangles are simple beams, in the case of the molecular level networks they are two benzene rings joined together by an acetylene chain. In such systems, it is primarily the acetylene chains,

1 Grima, Attard *et al.* (2008)

2
3 especially the longer ones, which behaves in a similar way to beams, and hence, in the
4
5 smaller systems, the deviations from the idealised scenario of a Poisson's ratio of -1 is
6
7 more significant thus contributing to the observed trend in the Poisson's ratio of $2A -$
8
9 $2C$. Furthermore it is important to note that the molecular level systems are
10
11 characterised by non-bond interactions which caused the different beams in the
12
13 systems to interact with each other. Such non-bond interactions are inversely
14
15 proportional r^k where r is the separation of the two interacting atoms, i.e. the extent of
16
17 interactions increases as the separation between the atoms involved decreases. This
18
19 will result in a scenario where the denser systems will have more of these non-bond
20
21 interactions per unit volume than the less dense systems thus, once again, resulting in
22
23 greater deviations from the idealised scenario of a Poisson's ratio of -1 in the smaller
24
25 systems when compared to the larger systems thus resulting All this results in the
26
27 observed trend in the Poisson's ratio of $2A - 2C$, where we find that $2A$ (the smaller
28
29 system) being the least auxetic and $2C$ (the larger less dense system) being the most
30
31 auxetic.
32
33
34
35
36
37
38
39
40

41 It is also interesting to note that although all the 'polycalixes' are auxetic, they do not
42
43 have an in-plane on axis Poisson's ratio of -1 as predicted by the idealised model[8].
44
45 These discrepancies may be explained using similar arguments, i.e. that the smaller
46
47 systems deviate more from the idealised model they are meant to mimic than the
48
49 larger systems. In particular, as explained elsewhere [8] we note that the idealised
50
51 'egg-rack / umbrella' model is not a very accurate representation of the 'double calix'
52
53 systems. In fact we note that these systems bear a greater resemblance to structures
54
55 whose joints are replaced by a rhombic units (see [8] for a more detailed discussion
56
57 and illustration) in which case we can identify two deformation mechanisms when the
58
59
60

Grima, Attard *et al.* (2008)

1
2
3
4 system is subjected to an external load. The first of these mechanisms, which acts on
5
6 the 'arms' of the system, opens the structure, in a similar way to the opening of an
7
8 umbrella, to flatten out the whole structure, thereby contributing to a negative
9
10 Poisson's ratio. The second one is the deformation of the rhombi leading to a positive
11
12 Poisson's ratio. These two opposing mechanisms act concurrently so that the net
13
14 Poisson's ratios for 'polycalixes' are less negative than expected. The actual values of
15
16 the Poisson's ratio depend on the relative magnitude of the mechanisms which
17
18 depends on the relative size of the rhombi when compared to the arms (the larger the
19
20 rhombi, the more they contribute to the overall deformation). From this analysis one
21
22 we would expect that the smaller systems (where the rhombi are more predominant)
23
24 to be less auxetic than the larger systems (where the umbrella arms are more
25
26 predominant). This trend is in fact evident in results obtained in this study where 3A
27
28 is found to be much less auxetic than 3C.
29
30
31
32
33

34
35
36 If we now look at the in-plane off-axis moduli of these systems (see Fig. 5) we note
37
38 that whilst the moduli of the polytriangles are unaffected by the direction of loading,
39
40 those of the reflexynes and the polycalixes are characterised by a high degree of
41
42 anisotropy. In particular we note that the high Young's moduli observed in the
43
44 reflexyne for on-axis loading decrease sharply for loading off-axis to values which are
45
46 about a fifth of their on-axis values. Furthermore, it is interesting to note that the
47
48 highly auxetic polytriangles and polycalixes are very distinct from each other in the
49
50 sense that the in-plane moduli of the polytriangles are consistently higher than the in-
51
52 plane moduli of the polycalixes, despite the fact that the polycalixes are significantly
53
54 more dense than the polytriangles (see Table 1). All this suggests that the
55
56 polytriangles may be better suited than the other networks, particularly the reflexynes,
57
58
59
60

1 Grima, Attard *et al.* (2008)

2
3 in applications which simultaneously require low density, high auxeticity, high
4 stiffness and/or isotropy in the in-plane properties.
5
6
7

8
9
10 Although the results on the re-entrant honeycombs presented here may *prima facie*
11 appear as surprising, particularly in view of the fact that the re-entrant shape is so
12 closely associated with auxetic behaviour, it is important to note that this lack of off-
13 axis auxeticity in ‘flexing re-entrant honeycombs’ is consistent with Gibson and
14 Ashby’s model of idealised honeycombs [53-54] and results from the fact that such
15 honeycombs are very weak in shear when compared to the uniaxial on-axis stretching,
16
17 In fact, as illustrated in Fig. 6a, the profile of Poisson’s ratio for a re-entrant
18 honeycombs made from ABS having dimensions t/l and h/l of 0.01 and 2
19 respectively (dimensions defined in Fig. 6b) is very similar to those of the molecular
20 level networks.
21
22
23
24
25
26
27
28
29
30
31
32
33

34 35 36 **Conclusion**

37
38 In this work we have fully characterised and compared the in-plane properties of
39 three types of hypothetical molecular polymeric networks which were predicted to
40 exhibit auxetic behaviour, in particular the polyphenylacetylene networks which, to a
41 first approximation, mimic the behaviour of ‘flexing re-entrant honeycombs’ or
42 ‘flexing rotating triangles’, and the polymers built from calix[4]arene building blocks.
43
44
45
46
47
48
49
50

51
52 We showed that these three types of systems exhibit very different mechanical
53 properties, with the polytriangles being *quasi* isotropic in the plane of the networks
54 whilst the other networks, particularly the reflexyne, are highly anisotropic.
55
56
57
58
59
60

1 Grima, Attard *et al.* (2008)

2
3 We also showed that although for many years it was assumed that auxetic behaviour
4 is primarily obtained from systems having re-entrant honeycomb characteristics, these
5 systems are not the best for obtaining auxetic behaviour due to the fact that they are
6 very weak in shear thus resulting in highly positive off-axis Poisson's ratios. In fact,
7 we showed that the polytriangles and the polycalixes are effectively more auxetic than
8 those based on the re-entrant model, with the polytriangles also benefiting from
9 higher shear moduli when compared to the polycalixes.
10
11
12
13
14
15
16
17
18
19
20
21
22
23

24 We hope that the comparison presented here will be of use to scientists working in the
25 design and synthesis of such molecular level auxetics by providing them with an
26 'ordered list' of systems that are most likely to exhibit auxetic behaviour, and also by
27 giving them a better insight into the stiffness that these systems are likely to have.
28
29
30
31
32
33
34
35

36 **Acknowledgements**

37
38 The financial support of the Malta Council for Science and Technology and of the
39 Malta Government Scholarship Scheme (Grant Number ME 367/07/17 awarded to
40 Daphne Attard) is gratefully acknowledged. The authors are also very grateful to
41 Accelrys Inc. for the assistance they provided.
42
43
44
45
46
47
48
49
50
51
52
53
54
55
56
57
58
59
60

1
2
3
4
5
6
7
8
9
10
11
12
13
14
15
16
17
18
19
20
21
22
23
24
25
26
27
28
29
30
31
32
33
34
35
36
37
38
39
40
41
42
43
44
45
46
47
48
49
50
51
52
53
54
55
56
57
58
59
60

Grima, Attard *et al.* (2008)

Reference:

- [1] K.E. Evans, M.A. Nkansah, I.J. Hutchinson, S.C. Rogers. Molecular network design. *Nature*, **353**, 124 (1991).
- [2] R. Lakes. Foam structures with a negative Poisson's ratio. *Science*, **235**, 1038 (1987).
- [3] S. P. Timoshenko, J. N. Goodier. *Theory of Elasticity* 3rd ed. McGraw-Hill, New York (1970).
- [4] A. Alderson. A triumph of lateral thought. *Chem. Ind.*, **10**, 384 (1999).
- [5] A. Alderson, P. J. Davies, M. R. Williams, K. E. Evans, K. L. Alderson, J. N. Grima. Modelling of the mechanical and mass transport properties of auxetic molecular sieves: An idealised organic (polymeric honeycomb) host-guest system. *Molecular Simulation*, **31**, 897 (2005).
- [6] J.N. Grima, K.E. Evans. Self expanding molecular networks. *Chem. Comm.*, **16**, 1531 (2000).
- [7] J.N. Grima, J.J. Williams, K.E. Evans. Networked calix[4]arene polymers with unusual mechanical properties. *Chem. Comm.*, **32**, 4065, (2005).
- [8] J.N. Grima, J.J. Williams, R. Gatt, K.E. Evans. Modelling of auxetic networked polymers built from calyx[4]arene building blocks. *Molecular Simulation*, **31**, 907 (2005).
- [9] K. E. Evans, A. Alderson, F. R. Christian. Auxetic two-dimensional polymer networks. An example of tailoring geometry for specific mechanical properties *J. Chem Soc. Faraday Trans*, **91**, 2671 (1995).
- [10] F. Scarpa, W.A. Bullough, P. Lumley. Trends in acoustic properties of iron particle seeded auxetic polyurethane foam. *P.I. Mech. Eng C - J. Mech. Engin. Sci.*, **218**, 241 (2004).

1
2
3
4
5
6
7
8
9
10
11
12
13
14
15
16
17
18
19
20
21
22
23
24
25
26
27
28
29
30
31
32
33
34
35
36
37
38
39
40
41
42
43
44
45
46
47
48
49
50
51
52
53
54
55
56
57
58
59
60

Grima, Attard *et al.* (2008)

- [11] K.E. Evans, M.A. Nkansah, I.J. Hutchinson. Auxetic foams - modeling negative Poisson's ratios. *Acta Metall. Mater.*, **42**, 1289 (1994).
- [12] C.W. Smith, J.N. Grima, K.E. Evans. A novel mechanism for generating auxetic behaviour in reticulated foams: Missing rib foam model. *Acta Materiala*, **48**, 4349 (2000).
- [13] J. N. Grima, A. Alderson, K. E. Evans. An alternative explanation for the negative Poisson's ratio in auxetic foams. *J. Phys. Soc. Jpn.*, **74**, 1341 (2005).
- [14] R.S. Lakes, K. Elms. Indentability of conventional and negative Poisson's ratio foams. *J. Compos. Mater.*, **27**, 1193 (1993).
- [15] N. Chan, K. E. Evans. Indentation resilience of conventional and auxetic foams. *J. Cell. Plast.*, **34**, 231 (1998).
- [16] J. B. Choi, R. S. Lakes. Nonlinear analysis of the Poisson's ratio of negative Poisson's ratio foams. *J. Compos. Mater.*, **29**, 113 (1995).
- [17] A. Yeganeh-Haeri, D. J. Weidner, J. B. Parise. Elasticity of alpha-cristobalite – a silicon dioxide with a negative Poisson's ratio. *Science*, **257**, 650 (1992).
- [18] N. R. Keskar, J. R. Chelikowsky. Negative Poisson ratios in crystalline SiO₂ from 1st-principles calculations. *Nature*, **358**, 222 (1992).
- [19] A. Alderson, K.L. Alderson, K.E. Evans, J.N. Grima, M. Williams. Modelling of Negative Poisson's Ratio Nanomaterials: Deformation Mechanisms, Structure - Property Relationships and Applications. *J. Metastable Nanocryst. Mater.*, **23**, 55 (2005).
- [20] A. Alderson, K. E. Evans. Rotation and dilation deformation mechanisms for auxetic behaviour in the alpha-cristobalite tetrahedral framework structure. *Phys. Chem. Miner.*, **28**, 711 (2001).

1
2
3
4
5
6
7
8
9
10
11
12
13
14
15
16
17
18
19
20
21
22
23
24
25
26
27
28
29
30
31
32
33
34
35
36
37
38
39
40
41
42
43
44
45
46
47
48
49
50
51
52
53
54
55
56
57
58
59
60

Grima, Attard *et al.* (2008)

- [21] A. Alderson, K.L. Alderson, K.E. Evans, J.N. Grima, M.R. Williams, P.J. Davies. Modelling the deformation mechanisms, structure-property relationships and applications of auxetic nanomaterials. *Phys. Status Solidi B*, **242**, 499 (2005).
- [22] J.N. Grima, R. Gatt, A. Alderson, K.E. Evans. On the origin of auxetic behaviour in the silicate α -cristobalite. *J. Mater. Chem.*, DOI: 10.1039/b508098c (2005).
- [23] H. Kimizuka, S. Ogata, Y. Shibutani. Atomistic characterization of structural and elastic properties of auxetic crystalline SiO₂. *Phys. Status Solidi B*, **244**, 900, (2007).
- [24] H. Kimizuka, H. Kaburaki, Y. Kogure. Mechanism for negative Poisson ratios over the α - β transition of Cristobalite, SiO₂: A Molecular-Dynamics Study. *Phys. Rev. Lett.*, **84**, 5548 (2000).
- [25] A. Alderson, K. E. Evans. Molecular origin of auxetic behavior in tetrahedral framework silicates. *Phys. Rev. Lett.*, **89**, 225503 (2002).
- [26] J.N. Grima, R. Gatt, A. Alderson, K.E. Evans. An alternative explanation for the negative Poisson's ratios in alpha-cristobalite. *Mater. Sci & Eng. A.*, **423** 219 (2006).
- [27] J.N. Grima, R. Jackson, A. Alderson, K.E. Evans. "Do zeolites have negative Poisson's ratios?" *Advanced Materials*, **12**, 1912 (2000).
- [28] J. N. Grima, V. Zammit, R. Gatt, A. Alderson, K. E. Evans. Auxetic behaviour from rotating semi-rigid units. *Phys. Status Solidi B*, **244**, 866, (2007).
- [29] J.N. Grima, R. Gatt, V. Zammit, J. J. Williams, K. E. Evans, A. Alderson, R. I. Walton. Natrolite: A zeolite with negative Poisson's ratios. *J. Appl. Phys.* **101**, 086102 (2007).
- [30] J. J. Williams, C. W. Smith, K. E. Evans, Z. A. D. Lethbridge, R. I. Walton. Off-Axis Elastic Properties and the Effect of Extraframework Species on Structural Flexibility of the NAT-Type Zeolites: Simulations of Structure and Elastic Properties. *Chem. Mater.*, **19**, 2423, (2007).

Grima, Attard *et al.* (2008)

- 1
2
3
4 [31] C. Sanchez-Valle, S. V. Sinogeikin, Z. A. D. Lethbridge, R. I. Walton, C. W.
5 Smith, K. E. Evans, J. D. Bass. Brillouin scattering study on the single-crystal
6 elastic properties of natrolite and analcime zeolites. *J. Appl. Phys.*, **98**, 053508
7 (2005).
8
9
10
11
12 [32] R.H. Baughman, D.S. Galvao. Crystalline networks with unusual predicted
13 mechanical and thermal-properties. *Nature*, **365**, 735 (1993).
14
15 [33] C.B. He, P.W. Liu, P.J. McMullan, A.C. Griffin. Toward molecular auxetics: Main
16 chain liquid crystalline polymers consisting of laterally attached paraquaterphenyls,
17 *Phys. Status Solidi B*, **242**, 576 (2005).
18
19 [34] C.B. He, P.W. Liu, A.C. Griffin. Toward negative Poisson ratio polymers through
20 molecular design, *Macromolecules*, **31**, 3145 (1998).
21
22 [35] P. Aldred, S.C. Moratti. Dynamic simulations of potentially auxetic liquid-crystalline
23 polymers incorporating swiveling mesogens. *Molecular Simulation*, **31**, 883 (2005).
24
25 [36] K.L. Alderson, K.E. Evans. Strain-dependent behaviour of microporous polyethylene
26 with a negative Poisson ratio. *J. Mater. Sci.* **28**, 4092 (1993).
27
28 [37] K.E. Evans, B.D. Caddock. Microporous materials with negative Poisson's ratios.2.
29 Mechanisms and interpretation. *J. Phys. D: Appl. Phys.*, **22**, 1877 (1989).
30
31 [38] R.H. Baughman, J.M. Shacklette, A.A. Zakhidov, S. Stafstrom. Negative Poisson's
32 ratios as a common feature of cubic metals. *Nature*, **392**, 362 (1998).
33
34 [39] A. Alderson, K. E. Evans. Microstructural modeling of auxetic microporous
35 polymers. *J. Mater. Sci.*, **30**, 3319 (1995).
36
37 [40] A. Alderson, K. E. Evans. Modelling concurrent deformation mechanisms in
38 auxetic microporous polymers. *J. Mater. Sci.*, **32**, 2797 (1997).
39
40 [41] G. Y. Wei. Design of auxetic polymer self-assemblies. *Phys. Stat. Sol. B.*, **242**,
41 742 (2005).
42
43
44
45
46
47
48
49
50
51
52
53
54
55
56
57
58
59
60

1
2
3
4
5
6
7
8
9
10
11
12
13
14
15
16
17
18
19
20
21
22
23
24
25
26
27
28
29
30
31
32
33
34
35
36
37
38
39
40
41
42
43
44
45
46
47
48
49
50
51
52
53
54
55
56
57
58
59
60

Grima, Attard *et al.* (2008)

- [42] J. N. Grima, A. Alderson, K. E. Evans. Auxetic behaviour from rotating rigid units. *Phys. Stat. Sol. B.*, **242**, 561 (2005).
- [43] K. V. Tretyakov, K. Wojciechowski. Poisson's ratio of simple planar 'isotropic' solids in two dimensions. *Phys. Stat. Sol. B.*, **244**, 1038 (2007).
- [44] R. F. Almgren. An isotropic three dimensional structure with Poisson's ratio = -1. *J. Elast.*, **15**, 427 (1985).
- [45] D. Prall, R. S. Lakes. Properties of a chiral honeycomb with a Poisson's ratio of -1. *Int. J. Mech. Sci.*, **39**, 305 (1997).
- [46] A. Spadoni, M. Ruzzene, F. Scarpa. Global and local linear buckling behavior of a chiral cellular structure. *Phys. Stat. Sol. B.*, **242**, 695 (2005).
- [47] K. W. Wojciechowski. Constant thermodynamic tension Monte Carlo studies of elastic properties of a two-dimensional systems of hard cyclic hexamers. *Molecular Physics*, **61**, 1247 (1987).
- [48] K. W. Wojciechowski, A. C. Branka. Negative Poisson ratio in a two-dimensional "isotropic" model. *Phys. Rev. A*, **40**, 7222 (1989).
- [49] K. W. Wojciechowski. Non-chiral, molecular model of negative Poisson ratio in two dimensions. *J. Phys. A. Math. Gen.*, **36**, 11765 (2003).
- [50] J.N. Grima, K.E. Evans. Auxetic behaviour from rotating squares. *J. Mater. Sci. Lett.*, **19**, 1563 (2000).
- [51] Y. Ishibashi, M. J. Iwata. A microscopic model of a negative Poisson's ratio in some crystals. *J. Phys. Soc. Jpn.*, **69**, 2702 (2000).
- [52] J. N. Grima, R. Gatt, A. Alderson, K. E. Evans. On the potential of connected stars as auxetic system. *Molecular Simulation*, **31**, 925, (2005).
- [53] L. J. Gibson, M. F. Ashby, G. S. Schajer, C. I. Robertson. The mechanics of two-dimensional cellular materials. *Proc. R. Soc. Lon. A*, **382**, 25 (1982).

1 Grima, Attard *et al.* (2008)

2
3 [54] L.J. Gibson, M.F. Ashby, Cellular Solids: Structure and Properties, Pergamon,
4 Oxford, 1988.

5
6
7 [55] J. N. Grima, K. E. Evans. Auxetic behaviour from Rotating Triangles. *J. Mater.*
8 *Sci.*, **41**, 3193 (2006).

9
10
11 [56] J. N. Grima, R. Gatt, P. S. Farrugia, A. Alderson, K. E. Evans. Auxetic cellular
12 materials and structures. *Proceedings of IMECE2005*, (2005).

13
14
15 [57] H. Sun, S. Mumby, J. Maple, A. Hagler. An ab-initio all-atom force-field for
16 polycarbonates. *J. Am. Chem. Soc.*, **116**, 2978 (1994).

17
18 [58] P. P. Ewald; *Ann. d. Physik*, 64, 253, (1921).

19
20 [59] J. F. Nye, *Physical Properties of Crystals*, Clarendon, Oxford, 1957.

21
22 [60] A. Hunter, J. Singh, J. Thornton. *pi-pi-interactions* – The geometry and energetics
23 of phenylalanine phenylalanine interactions in proteins. *J. Mol. Biol.*, **218**, 837
24 (1991).

25
26 [61] I.G. Masters, K.E. Evans. Models for the elastic deformation of honeycombs.
27 *Composite Structures*, **35**, 403 (1996).

Grima, Attard *et al.* (2008)

Figures

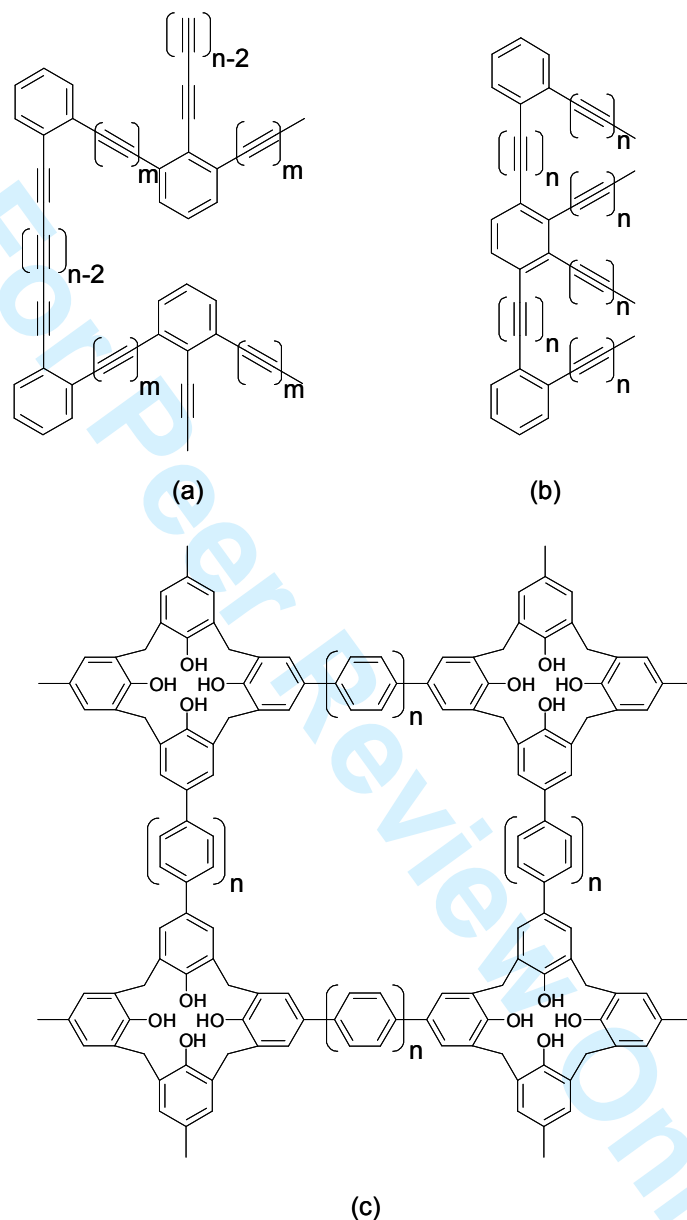


Fig. 1: An idealised 2D representation of the systems modelled in this paper: (a) the reflexynes 1A – C where for 1A, 1B and 1C $(m,n) = (1,4), (1,5)$ and $(1,6)$ respectively, (b) the polytriangles 2A – C where for 2A, 2B and 2C, $n = 3, 4$ and 5 respectively, and (c) the polycalixes 3A – C where for 3A, 3B and 3C, $n = 0, 1$ and 2 respectively.

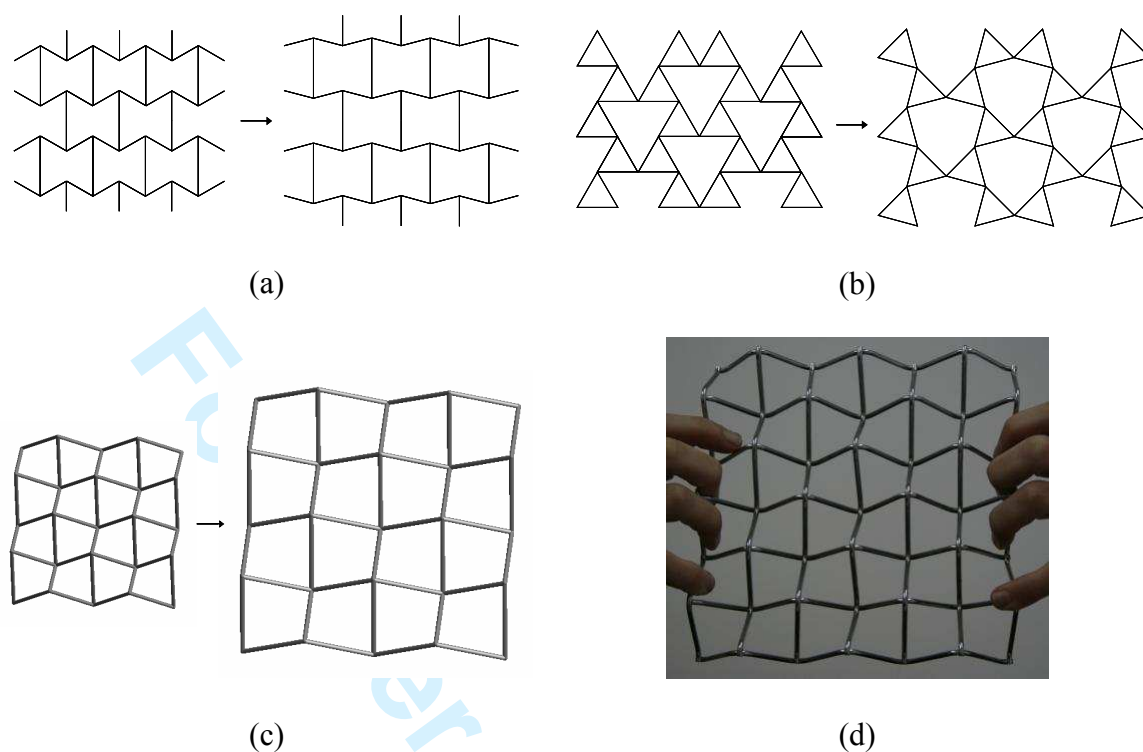
Grima, Attard *et al.* (2008)

Figure 2: (a-c) Examples of models/mechanisms exhibiting auxetic behaviour: (a) auxeticity from hinging re-entrant honeycombs; (b) auxeticity from rotating hinging triangles; (c) auxeticity from the ‘egg rack’ / ‘opening of an umbrella’ mechanism (The ‘egg rack’ on which this system is based is shown in (d)).

Animations of Fig. 2a – 2c are given as supplementary information in electronic format.

Grima, Attard *et al.* (2008)

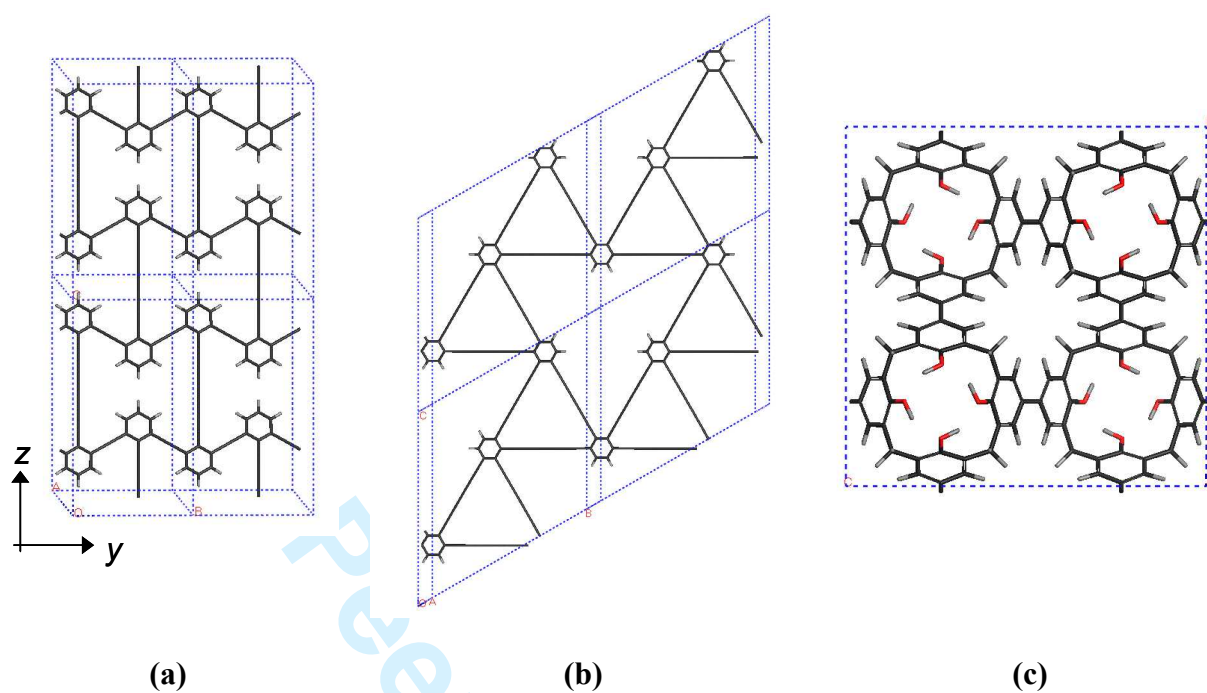


Figure 3: The projections in the YZ-plane of the minimum energy conformations of (a) 1A, (b) 2A and (c) 3A. Note that for clarity, the bond order is not shown.

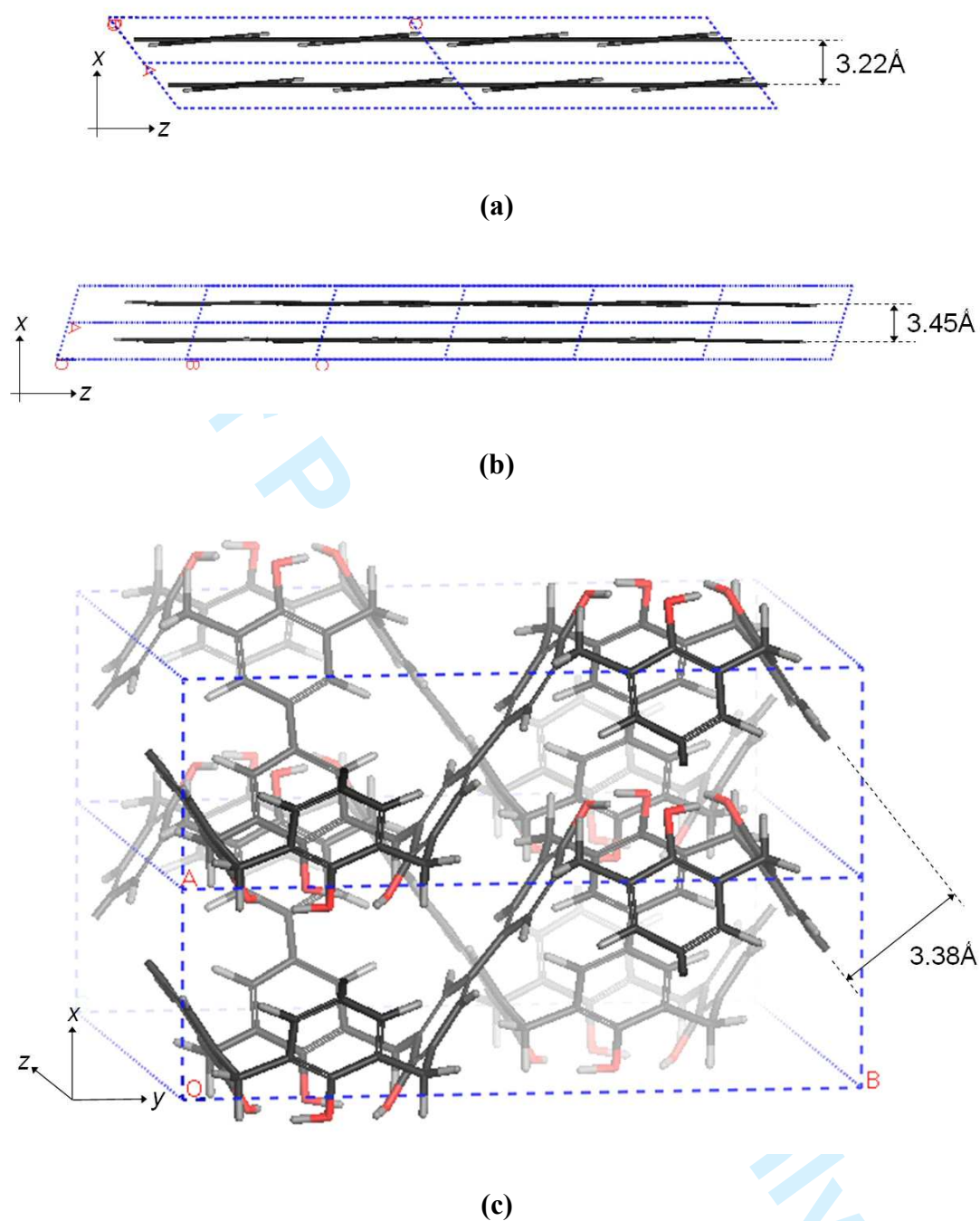
Grima, Attard *et al.* (2008)

Figure 4: Images showing the stacking down the 3rd dimension for (a) 1A, (b) 2A and (c) 3A. Note that in all cases, the stacking suggests that the π - π interactions are being well represented.

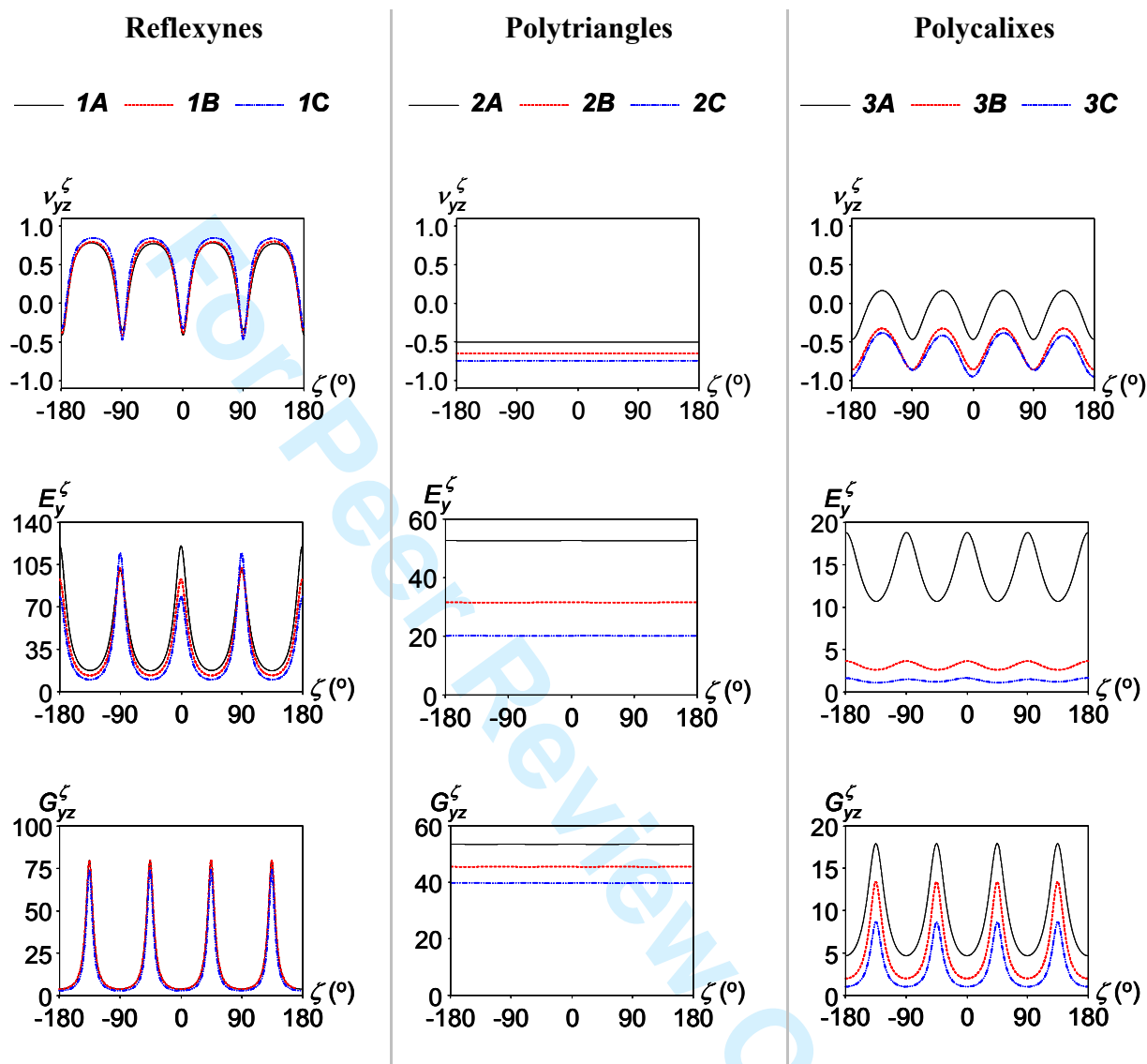
Grima, Attard *et al.* (2008)

Figure 5: Off-axis plots for the in-plane Poisson's ratios, ν_{yz} , Young's moduli E_y , and shear moduli G_{yz} for each of the network systems considered as obtained by the PCFF force-field.

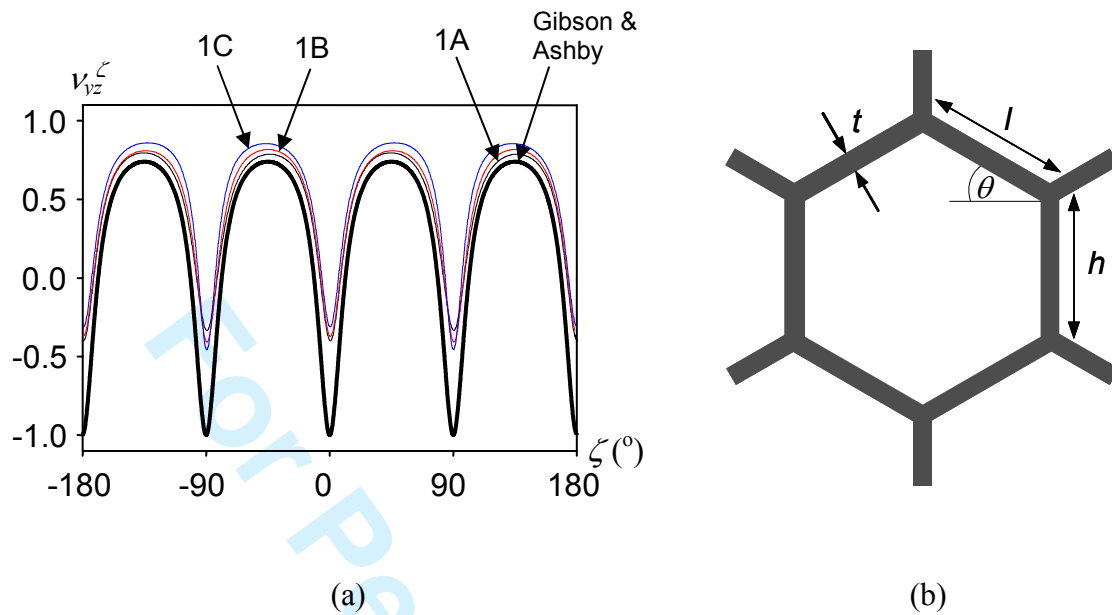
Grima, Attard *et al.* (2008)

Figure 6: (a) A comparison of the off-axis in-plane Poisson's ratio plots obtained in this study for the molecular networks 1A-C with those predicted through the analytical model of Gibson and Ashby [53, 54] for a structure made from ABS ($E_s = 2.206$ GPa) and with a $t:l$ ratio of 0.01, a $h:l$ ratio of 2 and a re-entrant angle of 30° (i.e. $\theta = -30^\circ$). Using these values, the on-axis Poisson's ratios were both found to be -1 while the Young's moduli were found to be 5.095MPa and the shear modulus 0.191MPa. (b) The geometrical parameters that define hexagonal honeycombs.

Grima, Attard *et al.* (2008)

Tables

| | Method | ν_{yz} | ν_{zy} | E_y (GPa) | E_z (GPa) | G_{yz} | Density (g/cm ³) |
|-----------|------------------------------|------------|------------|----------------|----------------|----------|---------------------------------|
| 1A | PCFF | -0.41 | -0.34 | 120.05 | 99.38 | 4.57 | 1.20 |
| | <i>Evans et al. [9]</i> | -0.29 | -0.29 | 124 | 110 | - | - |
| | <i>Alderson et al. [5]</i> | - | - | - | - | - | - |
| 1B | PCFF | -0.37 | -0.41 | 92.68 | 101.71 | 3.64 | 1.02 |
| | <i>Evans et al. [9]</i> | -0.29 | -0.39 | 95 | 116 | - | - |
| | <i>Alderson et al. [5]</i> | -0.33 | -0.39 | 94 | 110 | - | - |
| 1C | PCFF | -0.31 | -0.46 | 78.20 | 114.25 | 2.65 | 0.92 |
| | <i>Evans et al. [9]</i> | -0.22 | -0.42 | 84 | 140 | - | - |
| | <i>Alderson et al. [5]</i> | -0.28 | -0.44 | 80 | 124 | - | - |
| 2A | PCFF | -0.51 | -0.51 | 52.56 | 52.60 | 53.52 | 0.90 |
| | <i>Grima & Evans [6]</i> | -0.83 | -0.83 | - | - | - | - |
| 2B | PCFF | -0.65 | -0.65 | 31.51 | 31.48 | 45.50 | 0.75 |
| | <i>Grima & Evans [6]</i> | -0.90 | -0.90 | - | - | - | - |
| 2C | PCFF | -0.75 | -0.75 | 20.18 | 20.12 | 39.75 | 0.64 |
| | <i>Grima & Evans [6]</i> | -0.94 | -0.93 | - | - | - | - |
| 3A | PCFF | -0.47 | -0.47 | 18.79 | 18.79 | 4.61 | 1.42 |
| | <i>Grima et al. [8]</i> | -0.51 | -0.51 | 18.10 | 18.10 | - | - |
| 3B | PCFF | -0.86 | -0.86 | 3.65 | 3.65 | 1.95 | 1.10 |
| | <i>Grima et al. [8]</i> | -0.87 | -0.85 | 3.78 | 3.78 | - | - |
| 3C | PCFF | -0.95 | -0.87 | 1.67 | 1.52 | 0.99 | 0.89 |
| | <i>Grima et al. [8]</i> | -0.93 | -0.88 | 1.67 | 1.58 | - | - |

Table 1: Table 1: The on-axis mechanical properties of reflexynes (1A-1C), polytriangles (2A-2C) and ‘double calixes’ (3A-3C) obtained using the PCFF force-field found in Materials Studio compared to values obtained from literature.

Grima, Attard *et al.* (2008)

| | 1A | 1B | 1C | 2A | 2B | 2C | 3A | 3B | 3C |
|-----------------|------|------|------|-------|-------|-------|-------|-------|-------|
| $P_{aux}[YZ]$ | 0.17 | 0.16 | 0.13 | 1 | 1 | 1 | 0.58 | 1 | 1 |
| $\bar{\nu}[YZ]$ | 0.47 | 0.50 | 0.55 | -0.51 | -0.65 | -0.75 | -0.11 | -0.57 | -0.64 |

Table 2: The ‘auxetic probability’ $P_{aux}[YZ]$ and the ‘average in-plane Poisson’s ratio’

$\bar{\nu}[YZ]$ for the nine networks modelled.